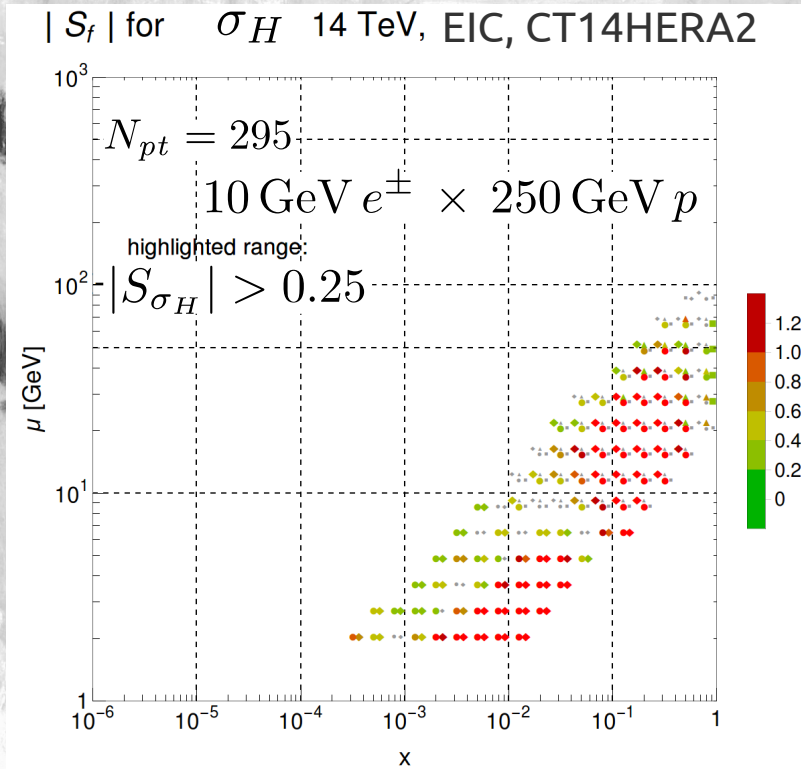


The **Electron Ion Collider** and its implications for high-energy phenomenology

10th International Workshop on Multiple Partonic Interactions at the LHC
Perugia, Italy

Thurs., Dec 13, 2018

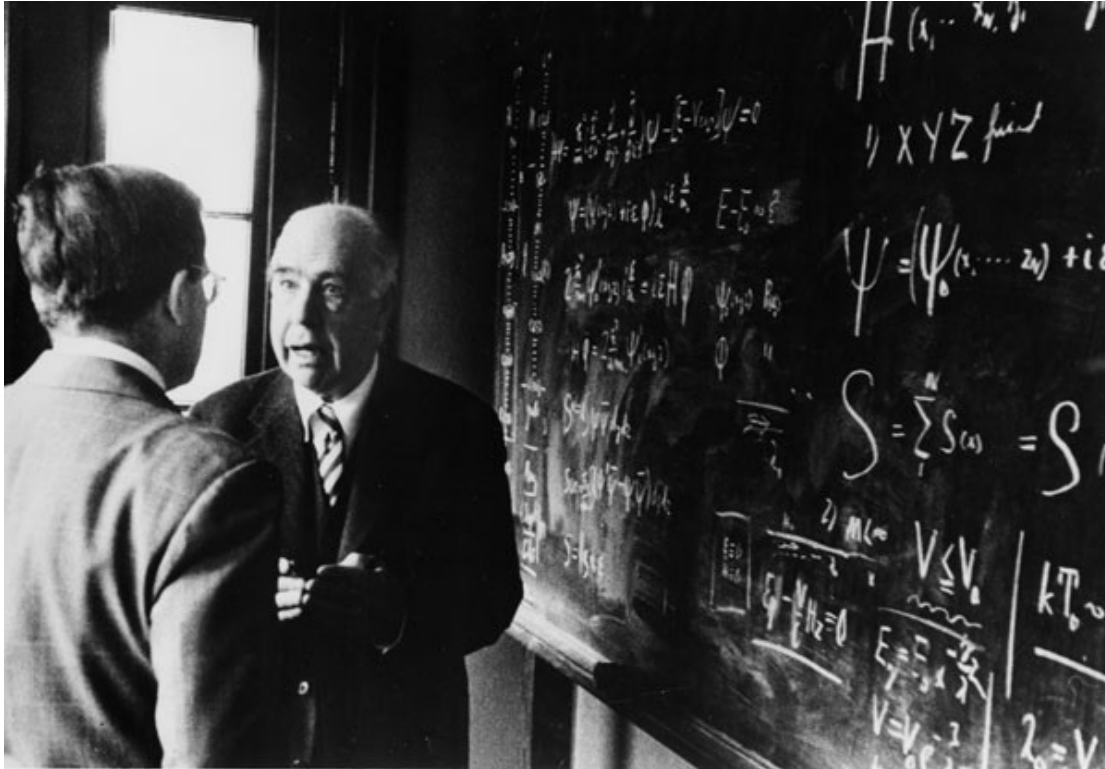


Tim Hobbs, Southern Methodist University & CTEQ
EIC Center at Jefferson Lab

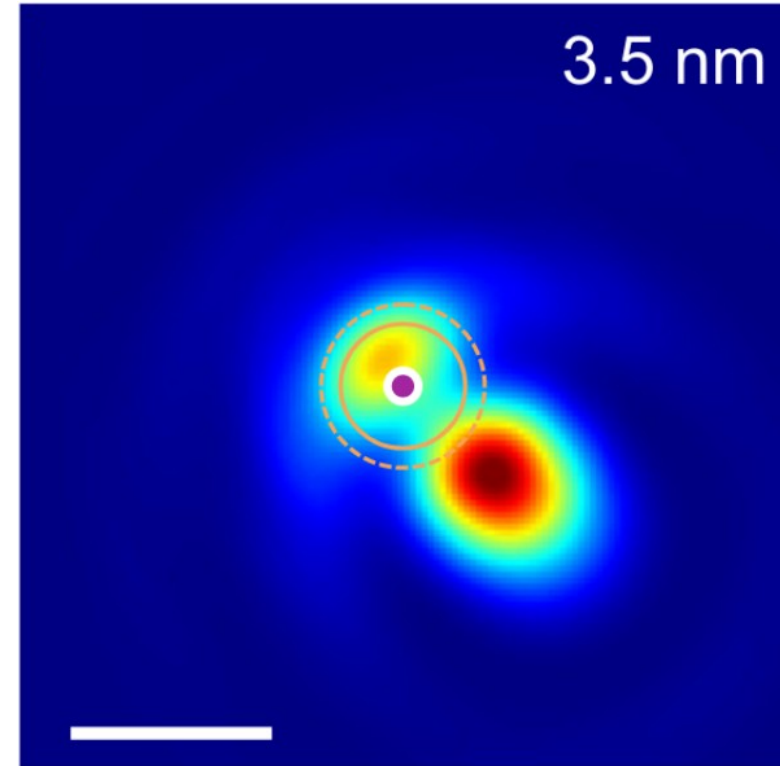
proton structure is today becoming a precision field

- the present moment is in many ways reminiscent of the situation in atomic structure theory in the early 20th Century:

Jeong et al., PRB93, 165140 (2016).



Niels with Aage at LANL.



Sr STEM simulated image

- much as the electronic structure of atomic matter has been mapped to high precision, we are entering an era of '**hadron tomography**'

... this is enshrined in the *2015 Nuclear Science Advisory Committee LRP*

➔ AND motivation for **EIC**, JLab12, LHeC, collider data analyses

EIC is an essential future tool for hadron tomography and QCD

[See Tues. talk by **Marco Radici** for project status and hadron physics motivations.]

The National
Academies of
SCIENCES
ENGINEERING
MEDICINE

THE NATIONAL ACADEMIES PRESS

This PDF is available at <http://nap.edu/25171>

SHARE



Summer 2018




An Assessment of U.S.-Based Electron-Ion Collider Science




“In summary, the committee finds a compelling scientific case for such a facility. The science questions that an EIC will answer are central to completing an understanding of atoms as well as being integral to the agenda of nuclear physics today.”

“Top-level” physics objectives – connecting the bulk properties of hadrons to a parton-level description:

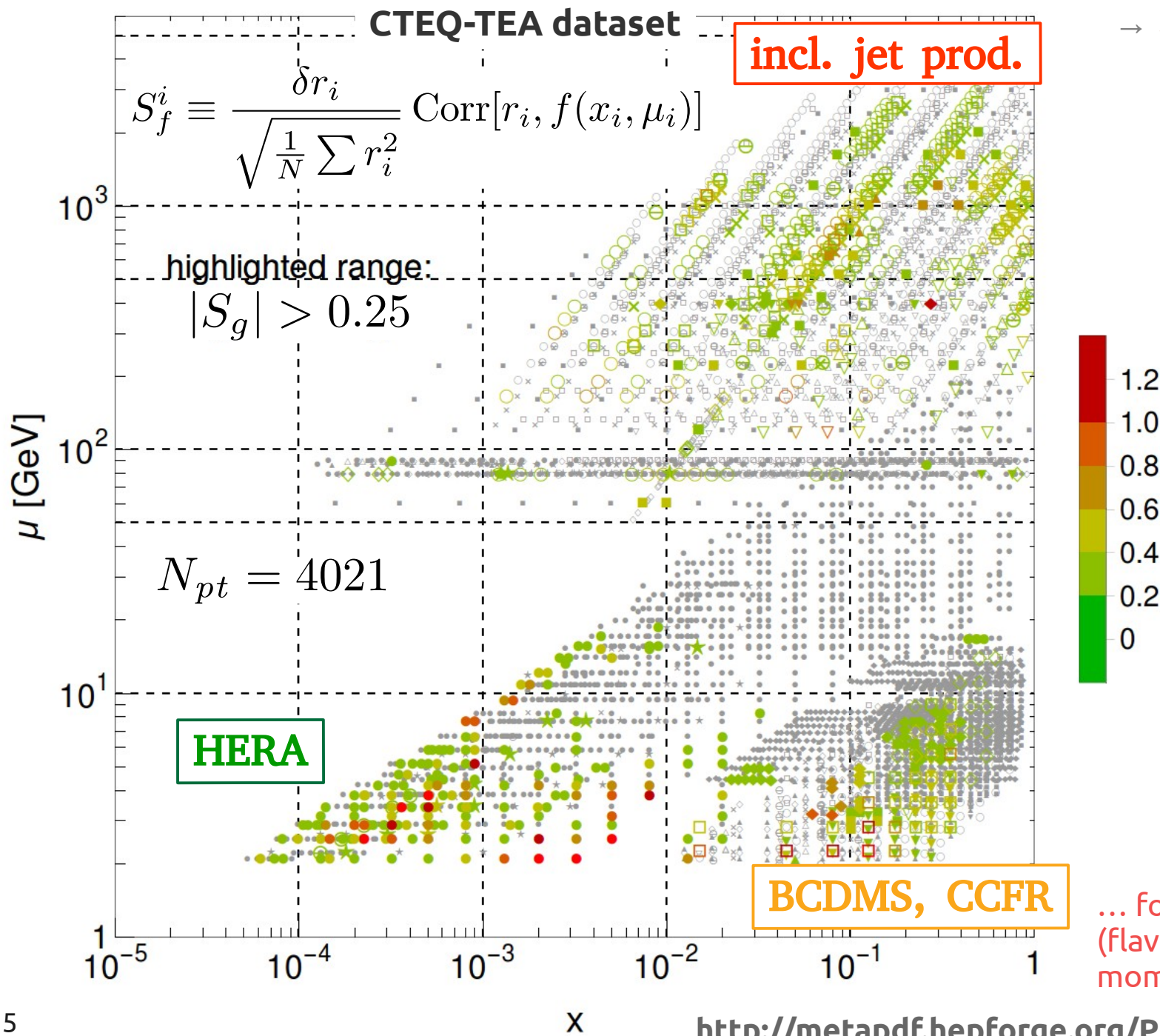
- the origin of nucleon mass and spin in partonic degrees of freedom
- understanding gluonic systems in the high density limit
- imaging the nucleon’s **multi-dimensional structure**

the capabilities that will allow EIC to address questions in QCD will also drive improvements in HEP

- EIC is a **very high luminosity** “femtoscope” – larger compared to HERA luminosities by a factor of $10^2 - 10^3$
- reach in center-of-mass energy, $10 \leq \sqrt{s} \leq \underline{100 \text{ GeV}}$ 
→ upgradeable to $\sqrt{s} \leq \underline{140 \text{ GeV}}$
- beam polarization of at least $\sim 70\%$ for e^- , p , light A

- as a generic scenario, we consider here the simulated impact of a machine with:
 $10 \text{ GeV } e^\pm$ on $250 \text{ GeV } p$ ($\sqrt{s} = 100 \text{ GeV}$)

 $\mathcal{L} = 100 \text{ fb}^{-1} e^-$ pseudodata 
 $\mathcal{L} = 10 \text{ fb}^{-1} e^+$ pseudodata  **NC/CC**
~year of data-taking

- EIC will map the few GeV **quark-hadron transition** region
- á la HERA, the combination of precision & kinematic coverage provide constraining ‘lever arm’ on QCD evolution
- QCD evolution: (**high x , low Q**) ↔ (**low x , high Q**)

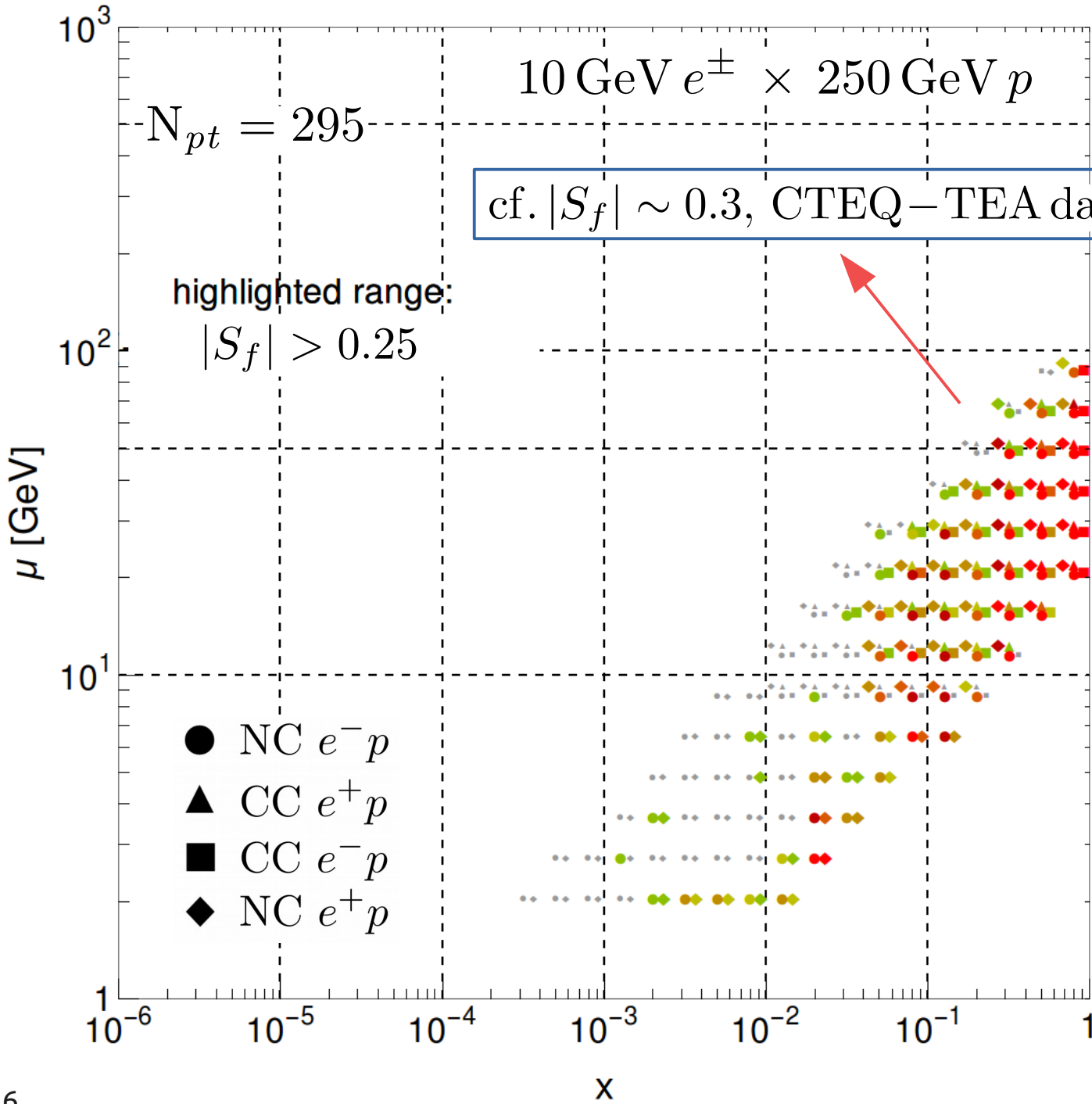


→ special thanks to **Bo-Ting Wang!**

- used in this talk, **PDFSENSE**: a tool to quantify and visualize the sensitivity of measured data to the PDFs (or PDF-dependent quantities)
- alternative to computationally costly QCD global analyses; yields a generalized correlation (the 'sensitivity') – a proxy for the expected impact in an actual fit

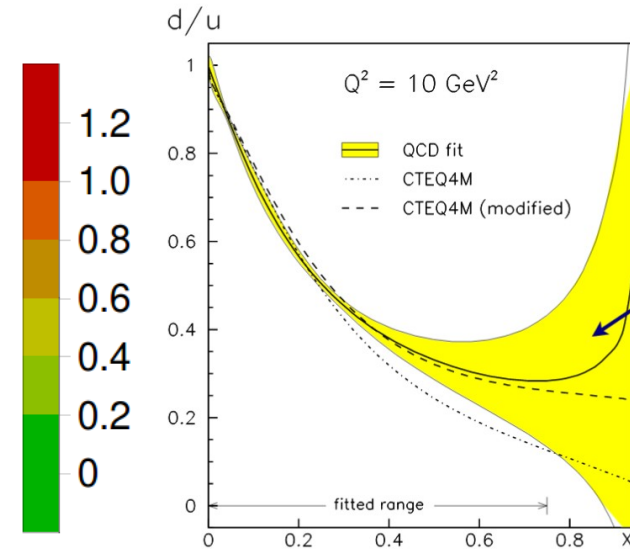
... for many other results (flavors, combinations, moments, cross sections):

$|S_f|$ for $d/u(x, \mu)$, CT14 HERA2 NNLO



- as a dedicated machine for hadron tomography, EIC can unravel stubborn issues in nucleon structure, *e.g.*, $d/u(x \approx 1)$

[a model discriminator]



- expected impact, or *sensitivity*, of EIC determined by examining pseudodata generated by fluctuating about CT14 theory predictions

the road ahead



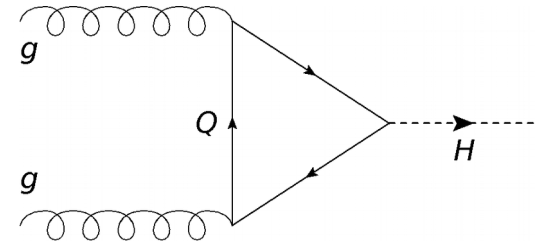
- the EIC will be a tool for **precise hadron tomography**
- BUT, also of importance to **HEP phenomenology!**
 - an EIC can be expected to enlighten:
 - high energy QCD – *e.g.*, the gluon and saturation
 - Higgs phenomenology
 - the electroweak sector
 - searches for New Physics
 - theory of multi-parton interactions
- the future: continuing to build the EIC physics case.

...examples...

QCD at high energies: an EIC and control over the gluon

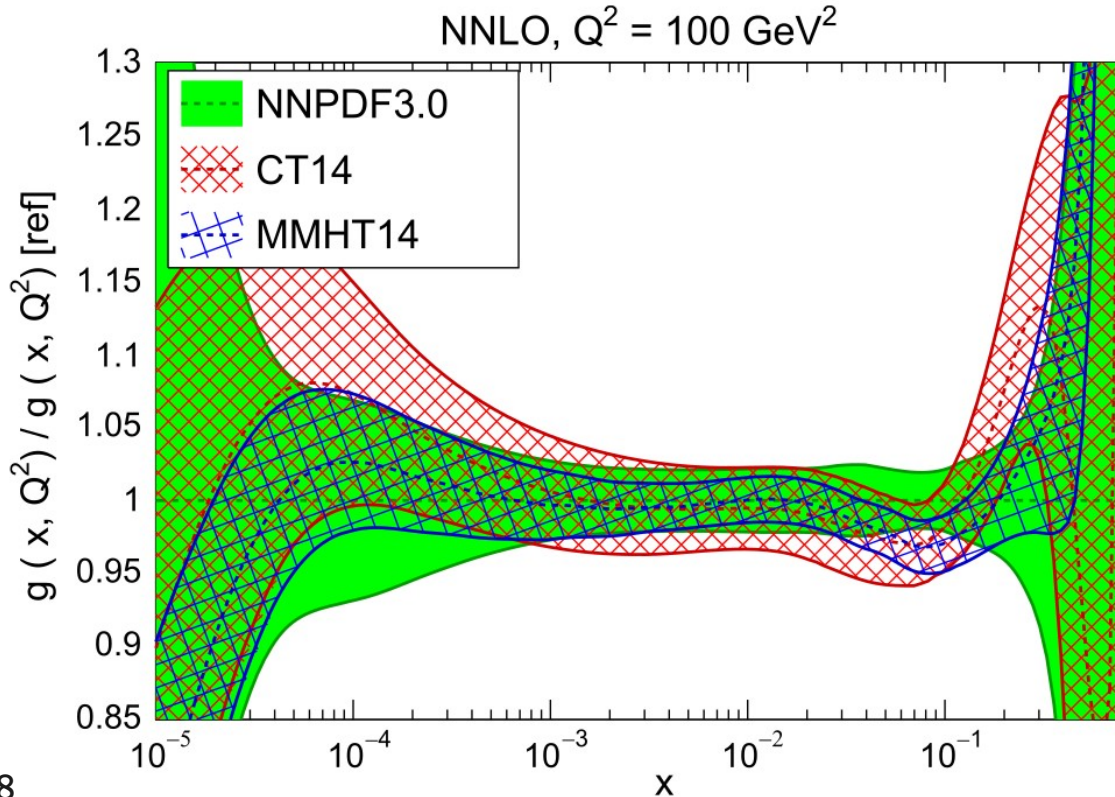
- the gluon is crucial to the mass of hadronic bound states, and $gg \rightarrow H$ is the dominant channel in Higgs production

BUT

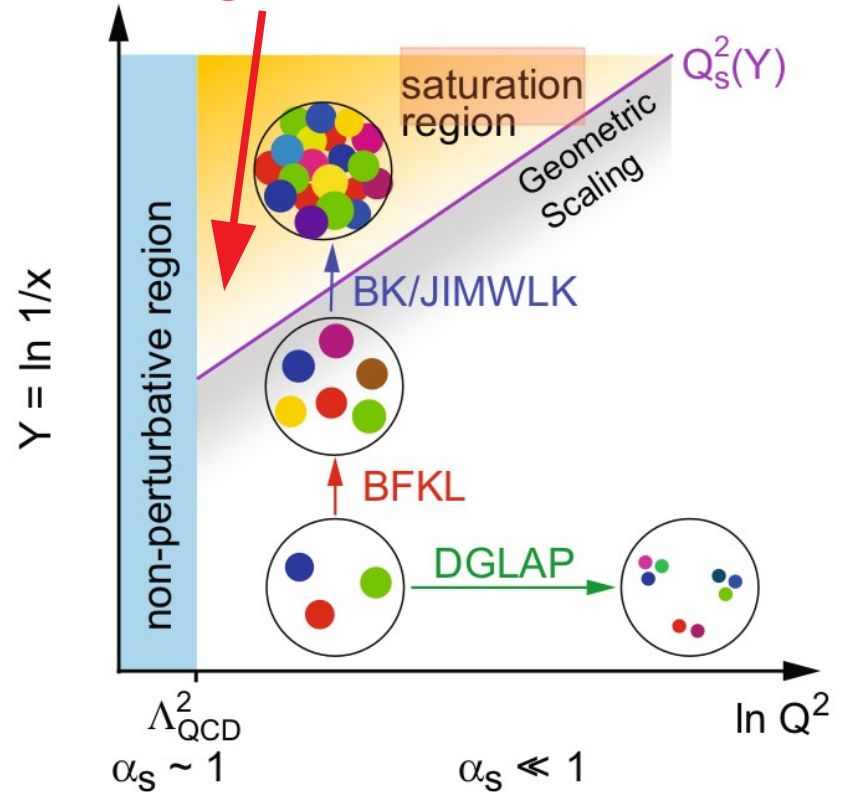


- while under better control at intermediate x , the collinear gluon PDF is poorly known toward the distribution endpoints, *i.e.*, $g(x, \mu)$ for $x \rightarrow 0, 1$

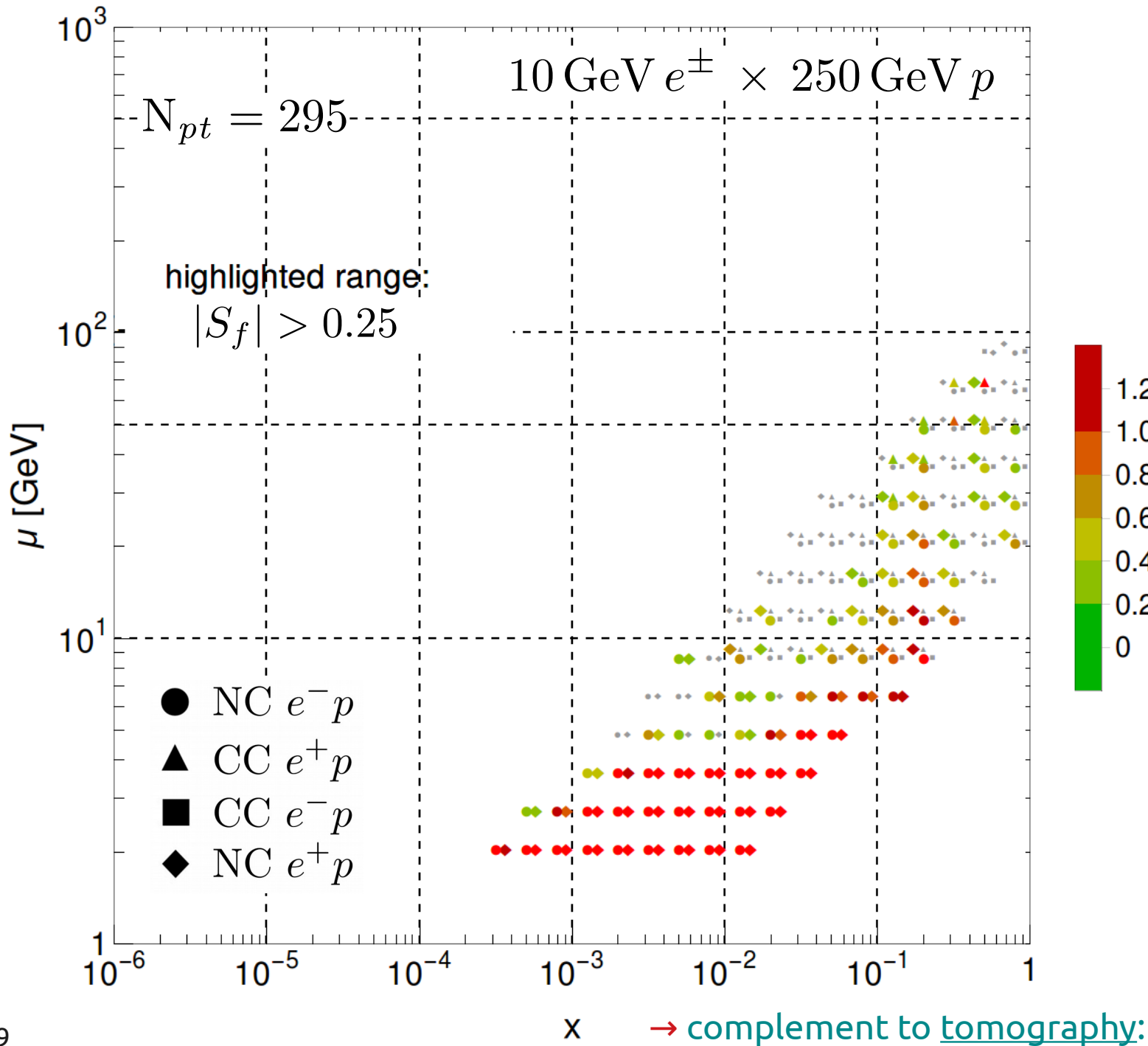
Rojo et al., J. Phys. G42, 103103 (2015).



can we begin to observe this transition?

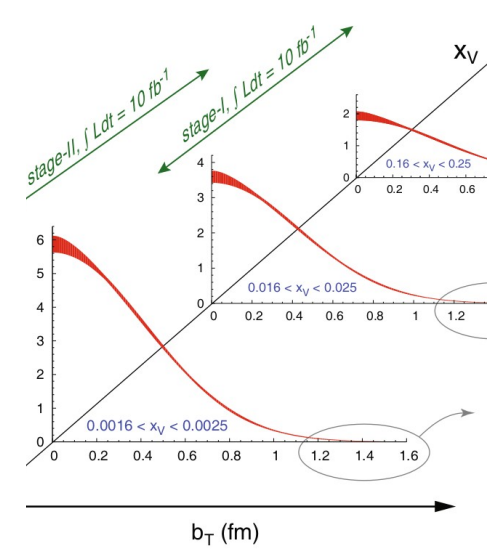


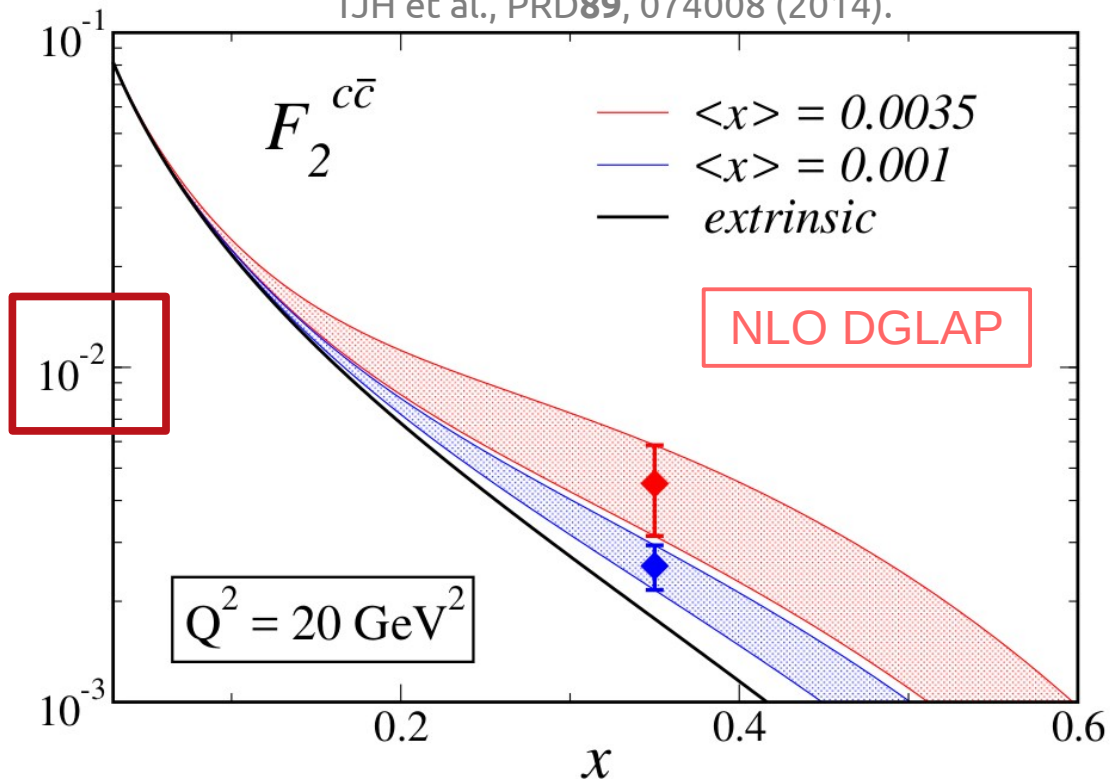
$|S_f|$ for $g(x, \mu)$ CT14 HERA2 NNLO



- an EIC will provide a sensitive probe to the gluon distribution – especially at low x
 $x \gtrsim 3 \times 10^{-4}$

- these constraints arise from high statistics neutral current data on $\sigma_{r,NC}^{e^\pm p}$



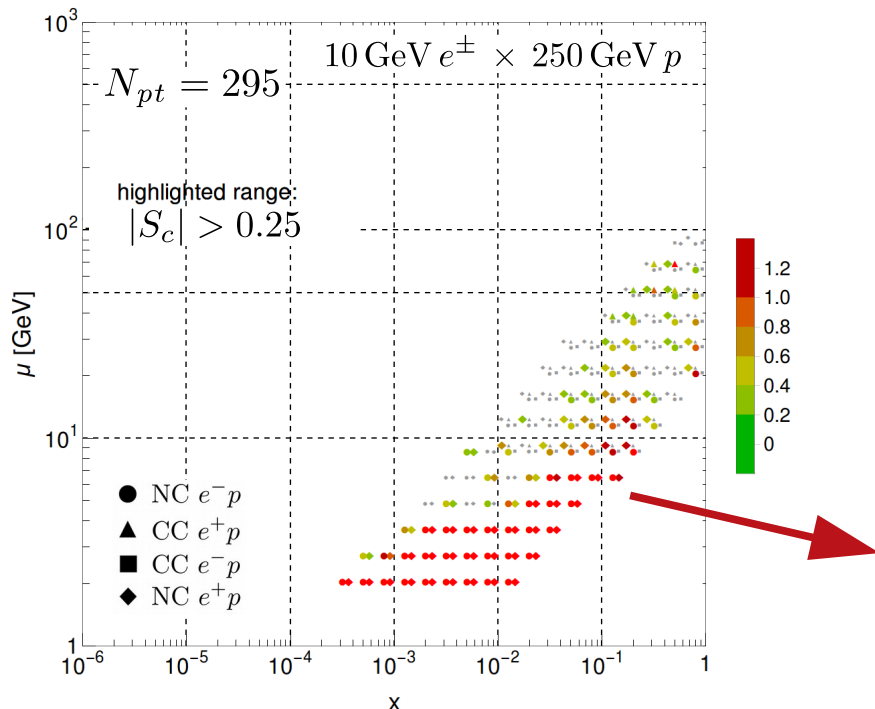


An EIC can finally resolve the NP nucleon charm question

- various models predict a nonperturbative (intrinsic) component to the nucleon structure function, but the normalization is small and undetermined

$$\langle x \rangle_{\text{IC}} = \int_0^1 dx x [c + \bar{c}](x, m_c^2) \lesssim 1 - 2\%$$

$|S_f|$ for $c(x, \mu)$, CT14 HERA2 NNLO



- the presence of a NP charm component has consequences for **heavy quark schemes, masses, and global analyses**

an EIC will measure very precisely in the ~few GeV, high x region in which typical NP charm signals are to be expected, à la EMC

Higgs production is now dominated by PDF and α_s uncertainties

- there remains considerable dependence (as large as $\sim 13\%$) upon PDF parametrization and running coupling

→ the situation is such that precision in Higgs phenom. is significantly **PDF-limited**

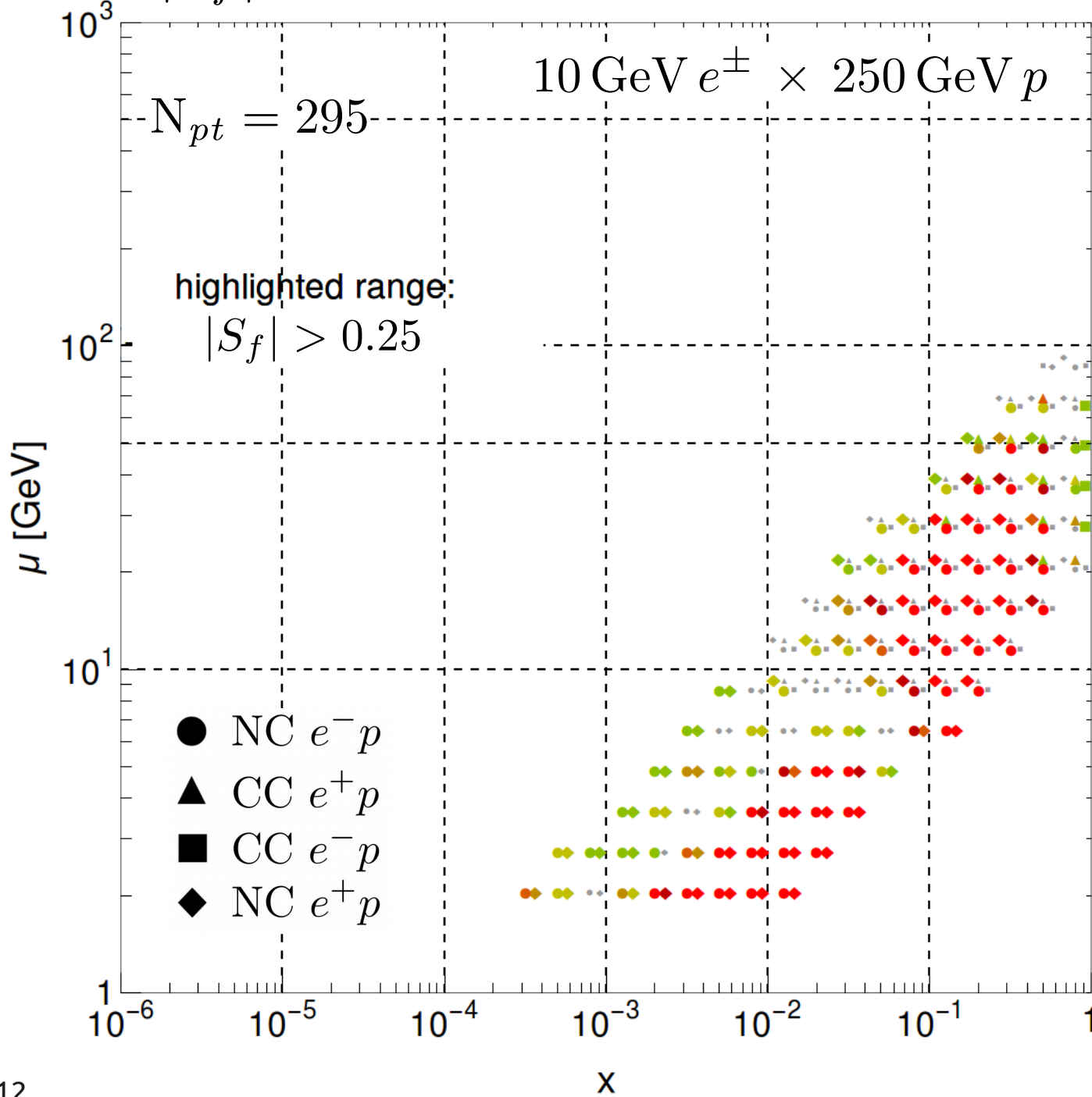
Accardi et al., EPJC**76**, 471 (2016).

PDF sets	$\sigma(H)^{\text{NNLO}}$ (pb) nominal $\alpha_s(M_Z)$	$\sigma(H)^{\text{NNLO}}$ (pb) $\alpha_s(M_Z) = 0.115$	$\sigma(H)^{\text{NNLO}}$ (pb) $\alpha_s(M_Z) = 0.118$
ABM12 [2]	39.80 ± 0.84	41.62 ± 0.46	44.70 ± 0.50
CJ15 [1] ^a	$42.45^{+0.43}_{-0.18}$	$39.48^{+0.40}_{-0.17}$	$42.45^{+0.43}_{-0.18}$
CT14 [3] ^b	$42.33^{+1.43}_{-1.68}$	$39.41^{+1.33}_{-1.56}$ (40.10)	$42.33^{+1.43}_{-1.68}$
HERAPDF2.0 [4] ^c	$42.62^{+0.35}_{-0.43}$	$39.68^{+0.32}_{-0.40}$ (40.88)	$42.62^{+0.35}_{-0.43}$
JR14 (dyn) [5]	38.01 ± 0.34	39.34 ± 0.22	42.25 ± 0.24
MMHT14 [6]	$42.36^{+0.56}_{-0.78}$	$39.43^{+0.53}_{-0.73}$ (40.48)	$42.36^{+0.56}_{-0.78}$
NNPDF3.0 [7]	42.59 ± 0.80	39.65 ± 0.74 (40.74 \pm 0.88)	42.59 ± 0.80
PDF4LHC15 [8]	42.42 ± 0.78	39.49 ± 0.73	42.42 ± 0.78

σ_H at NNLO and $\sqrt{s} = 13 \text{ TeV}$; $\mu_F = \mu_R = m_H$

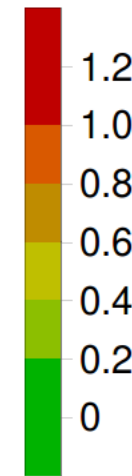
→ enhancing the discovery potential in the Higgs sector will require improving these uncertainties!

$|S_f|$ for σ_H , 14 TeV CT14 HERA2 NNLO

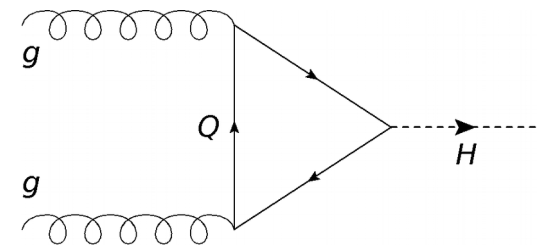


potentially strong impact on the Higgs sector

- the impact of an EIC upon the theoretical predictions for inclusive Higgs production arises from a very broad region of the kinematical space it can access



- impact rather closely tied to that of the integrated gluon PDF:

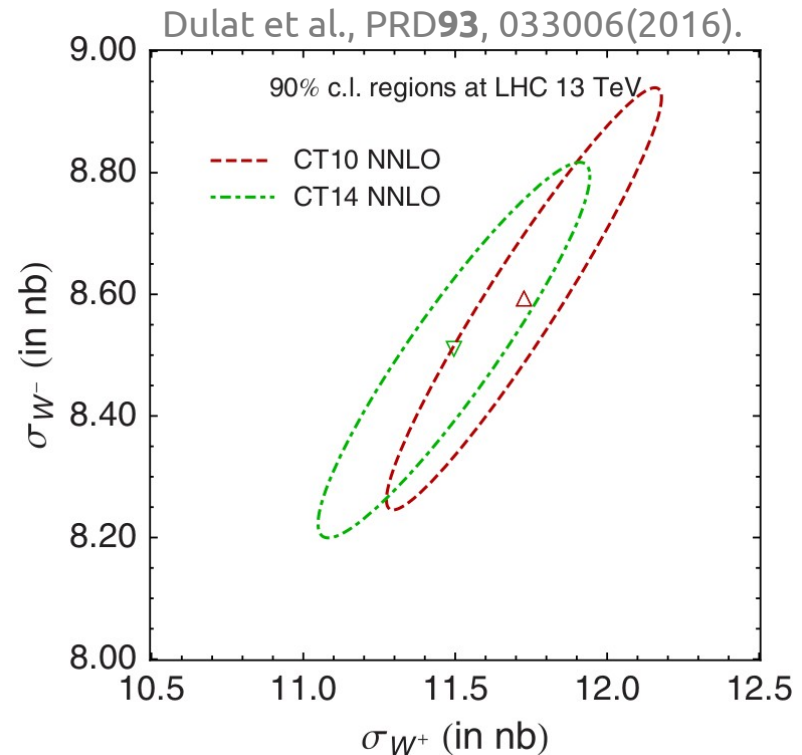
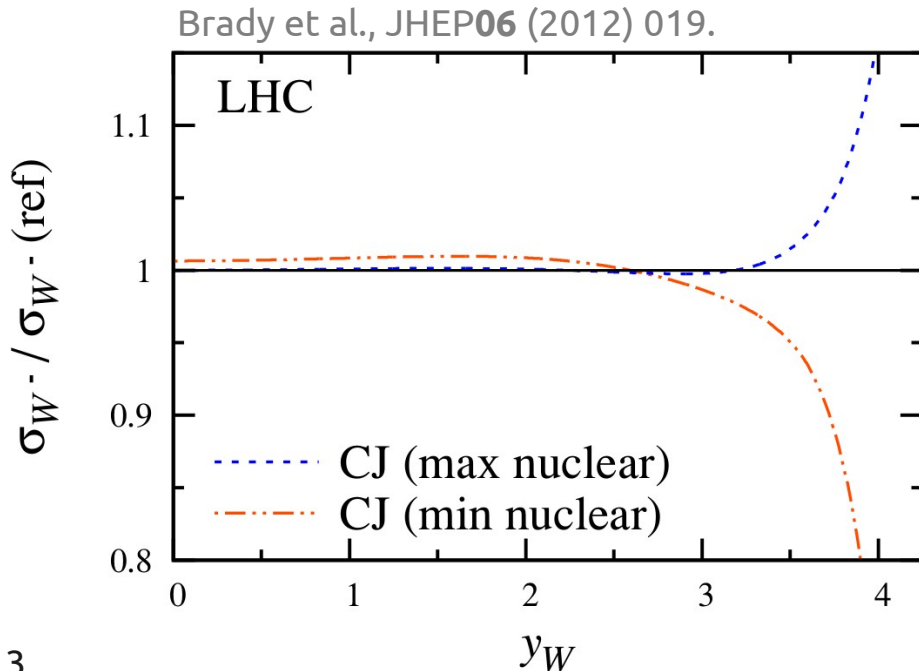


EIC and an era of (higher) precision **electroweak physics** (?)

- theory predictions for the production of gauge bosons are quite sensitive to the nucleon PDFs: *e.g.*, $d(x)$ at $x \sim 1$, which is poorly constrained

$$x_{1,2} = \frac{M}{\sqrt{s}} e^{\pm y}$$

$$\frac{d\sigma}{dy}(pp \rightarrow W^- X) = \frac{2\pi G_F}{3\sqrt{2}} x_1 x_2 \left(\cos^2 \theta_C \{d(x_1)\bar{u}(x_2) + \bar{u}(x_1)d(x_2)\} + \sin^2 \theta_C \{s(x_1)\bar{u}(x_2) + \bar{u}(x_1)s(x_2)\} \right)$$



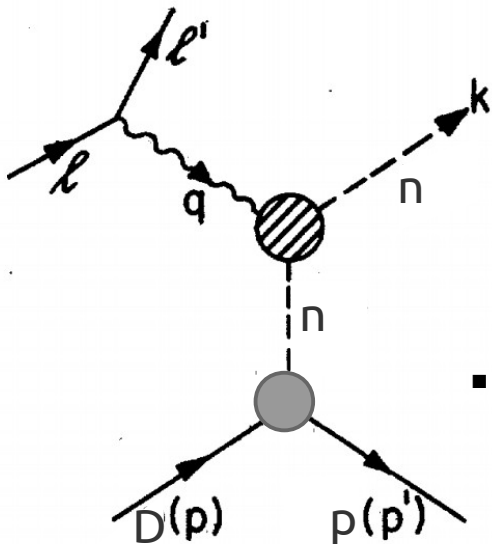
historically, extractions of $d(x)$, $x \rightarrow 1$ have depended on nuclear targets (and corrections!)

- in principle, a neutron target would allow the flavor separation needed to access $d(x, Q^2)$

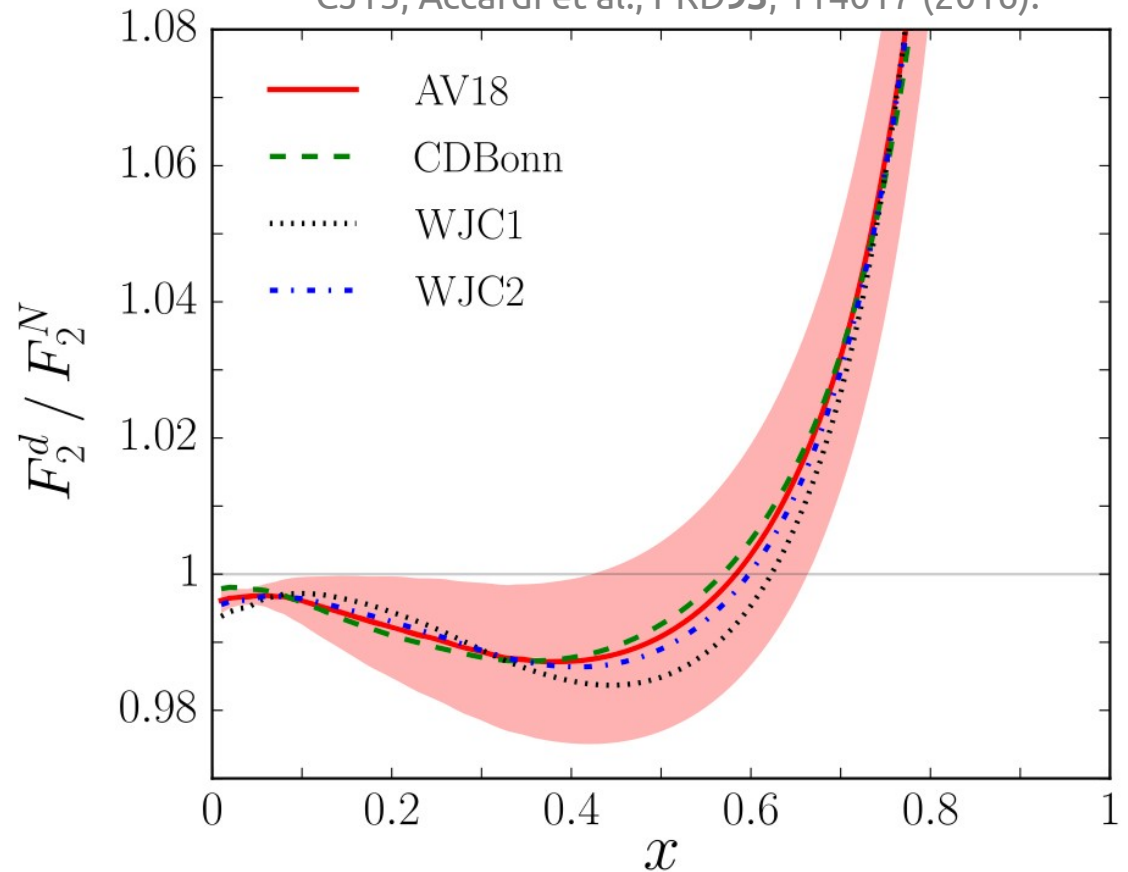
$$F_2^{e^- n} \sim x(4d + u)/9$$

— vs —

$$F_2^{e^- p} \sim x(4u + d)/9$$



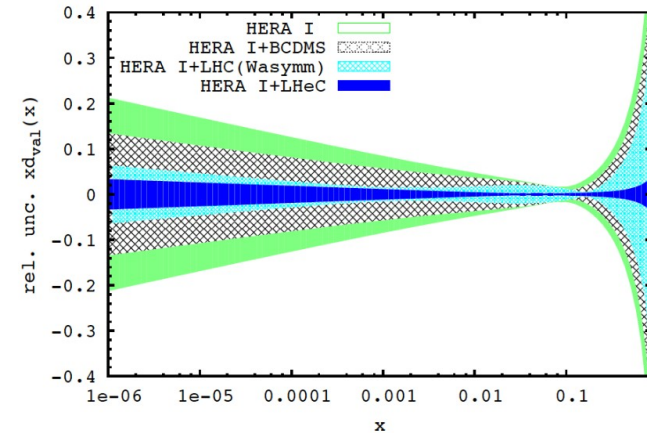
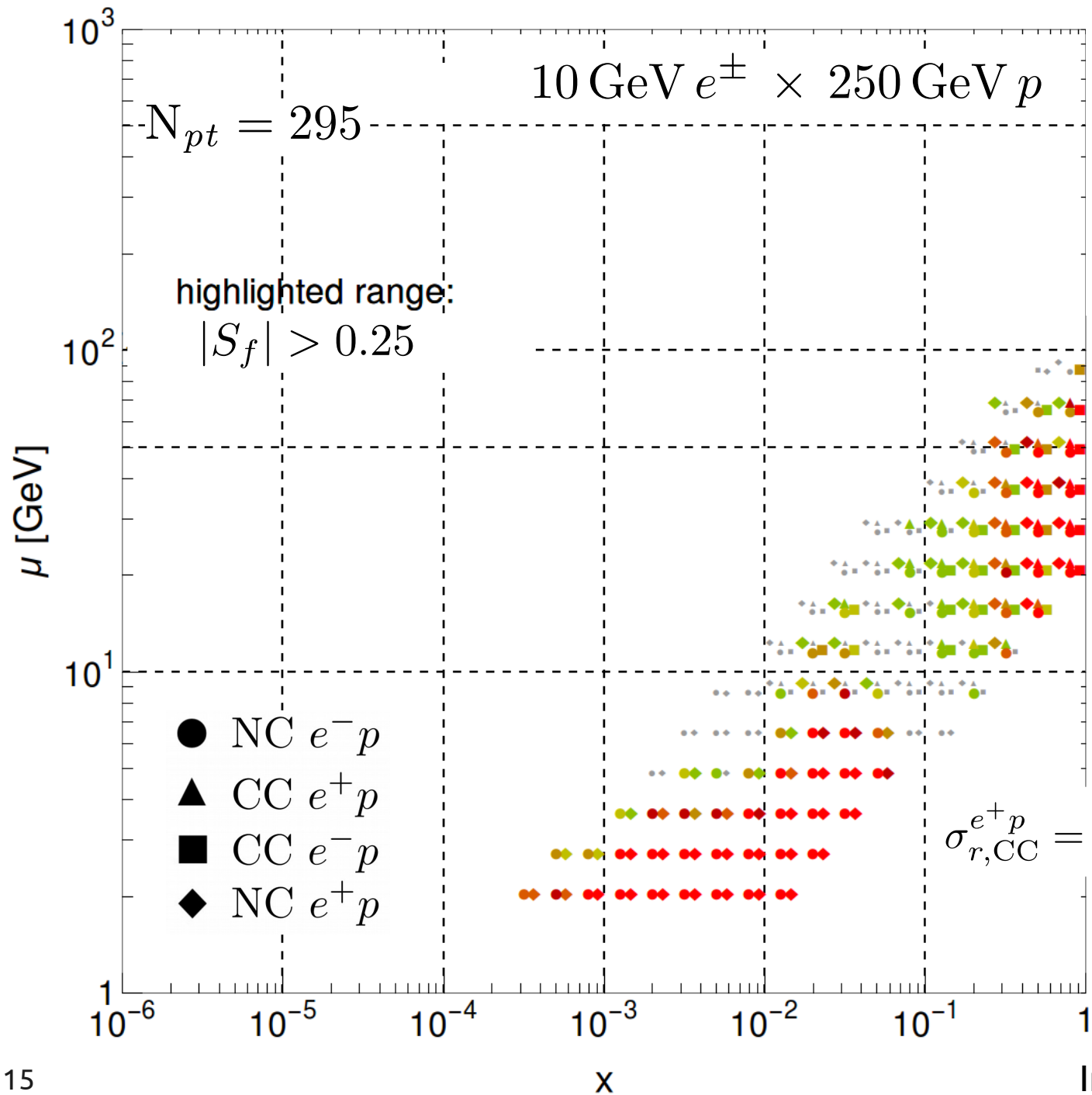
CJ15, Accardi et al., PRD93, 114017 (2016).



- BUT:** in the absence of a free neutron target, scattering from nuclei (e.g., the deuteron) is necessary

→ **nuclear corrections (Fermi motion) are sizable, especially for large x**

$|S_f|$ for $d(x, \mu)$ CT14 HERA2 NNLO



- an EIC affords **strong sensitivities without a nuclear target**; here, at both very high and very low x

for $x \rightarrow 1$

$$\sigma_{r,CC}^{e^+p} = \frac{Y_+}{2} W_2^+ \mp \frac{Y_-}{2} x W_3^+ - \frac{y^2}{2} W_L^+$$

$$\simeq [1 - y]^2 x(d + s)$$

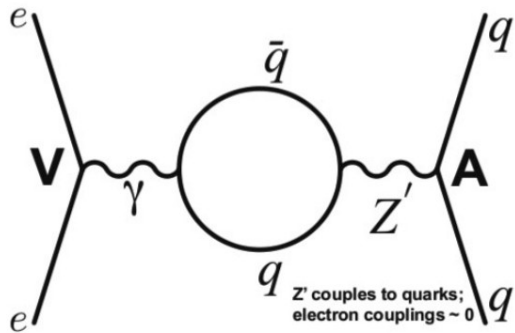
In the **LO quark-parton model**

the electroweak sector and **New Physics** searches at EIC

- if measured to sufficient precision, the quark-level electroweak couplings may be sensitive to an extended EW sector, e.g., Z'

$$\mathcal{L}^{\text{PV}} = \frac{G_F}{\sqrt{2}} \left[\bar{e} \gamma^\mu \gamma_5 e \left(C_{1u} \bar{u} \gamma_\mu u + C_{1d} \bar{d} \gamma_\mu d \right) + \bar{e} \gamma^\mu e \left(C_{2u} \bar{u} \gamma_\mu \gamma_5 u + C_{2d} \bar{d} \gamma_\mu \gamma_5 d \right) \right]$$

$$C_{1u} = -\frac{1}{2} + \frac{4}{3} \sin^2 \theta_W$$



- a unique strength of an EIC is its combination of very high precision and **beam polarization**, which allows the observation of **parity-violating helicity asymmetries**:

$$A^{\text{PV}} = \frac{\sigma_R - \sigma_L}{\sigma_R + \sigma_L} \quad (\text{R/L : } e^- \text{ beam helicities})$$

selects γ - Z interference diagrams!

TJH and Melnitchouk, PRD77, 114023 (2008).

$$A^{\text{PV}} = - \left(\frac{G_F Q^2}{4\sqrt{2}\pi\alpha} \right) (Y_1 a_1 + Y_3 a_3)$$

$$a_1 = \frac{2 \sum_q e_q C_{1q} (q + \bar{q})}{\sum_q e_q^2 (q + \bar{q})}$$

$$a_3 = \frac{2 \sum_q e_q C_{2q} (q - \bar{q})}{\sum_q e_q^2 (q + \bar{q})}$$

the electroweak sector and **New Physics** searches at EIC

- if measured to sufficient precision, the quark-level electroweak couplings may be sensitive to an extended EW sector, e.g., Z'

$$\mathcal{L}^{\text{PV}} = \frac{G_F}{\sqrt{2}} \left[\bar{e} \gamma^\mu \gamma_5 e \left(C_{1u} \bar{u} \gamma_\mu u + C_{1d} \bar{d} \gamma_\mu d \right) + \bar{e} \gamma^\mu e \left(C_{2u} \bar{u} \gamma_\mu \gamma_5 u + C_{2d} \bar{d} \gamma_\mu \gamma_5 d \right) \right]$$

$$C_{1u} = -\frac{1}{2} + \frac{4}{3} \sin^2 \theta_W$$

→ with sufficient precision, an EIC (which will be statistics-limited in these measurements) can extract $\sin^2 \theta_W$

- this measurement is potentially sensitive to the TeV-scale in a complementary fashion to energy-frontier searches!

TJH and Melnitchouk, PRD77, 114023 (2008).

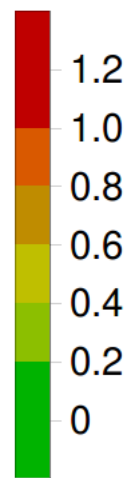
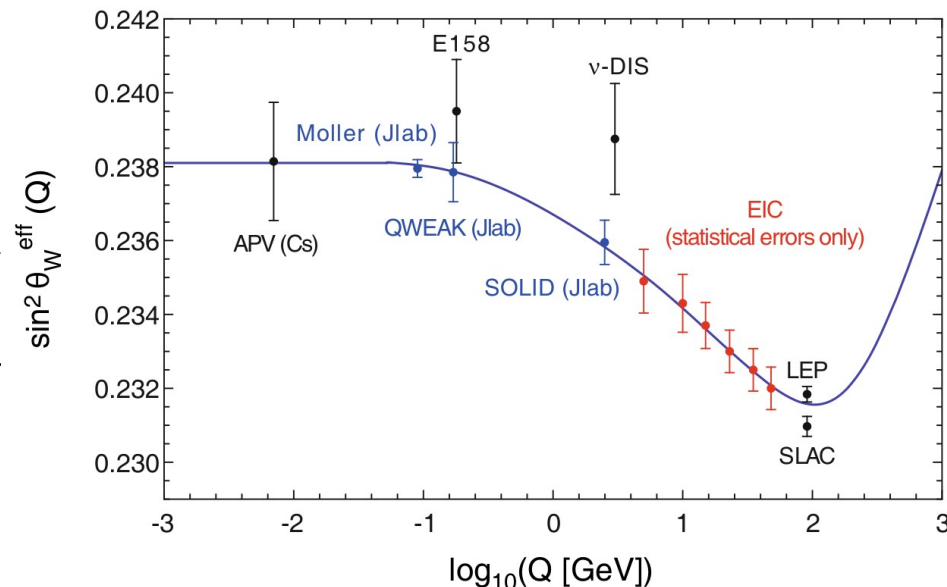
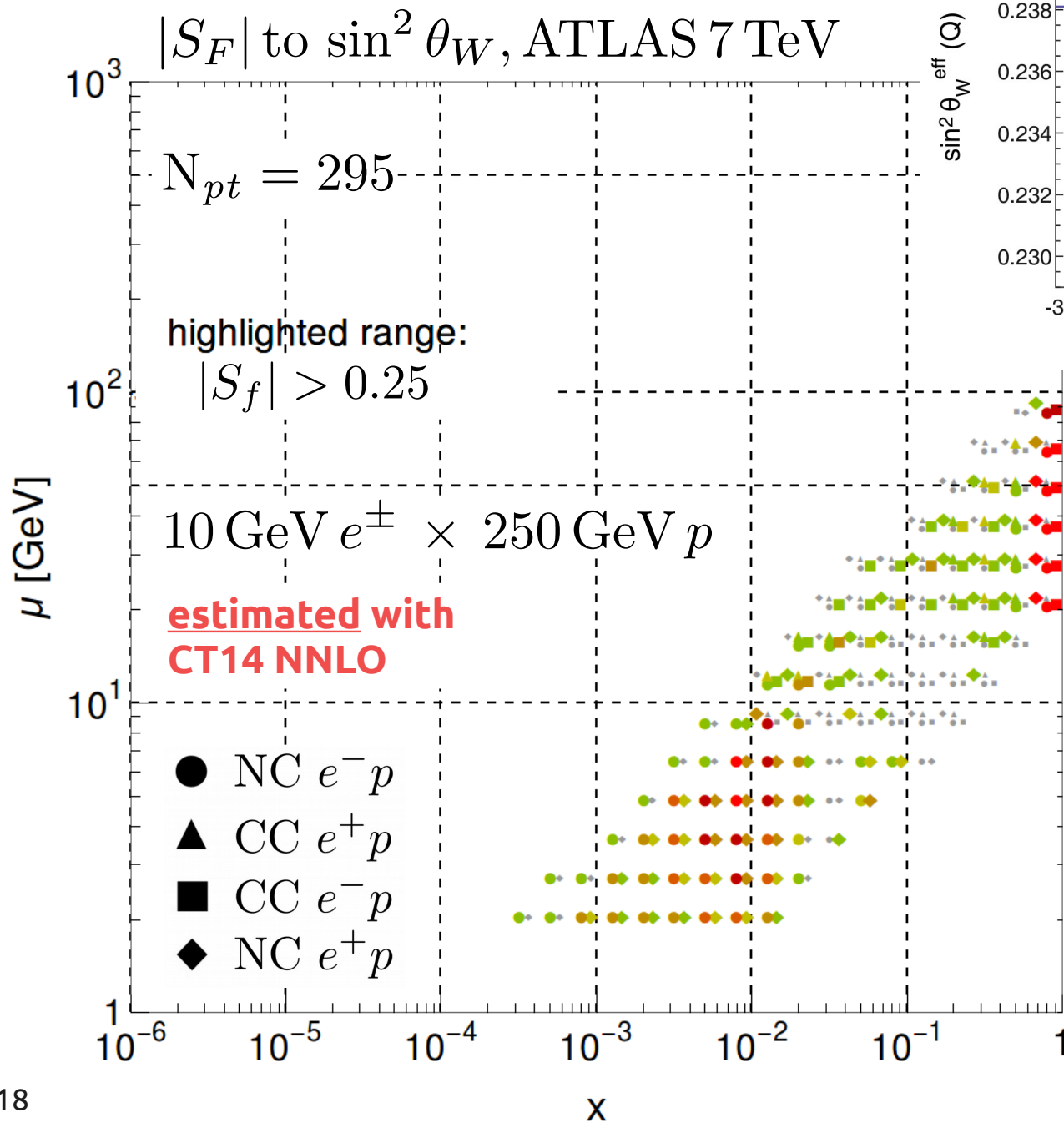
$$A^{\text{PV}} = - \left(\frac{G_F Q^2}{4\sqrt{2}\pi\alpha} \right) (Y_1 a_1 + Y_3 a_3)$$

$$a_1 = \frac{2 \sum_q e_q C_{1q} (q + \bar{q})}{\sum_q e_q^2 (q + \bar{q})}$$

$$a_3 = \frac{2 \sum_q e_q C_{2q} (q - \bar{q})}{\sum_q e_q^2 (q + \bar{q})}$$

N.B.: extractions are dependent upon knowledge of the PDFs

an EIC will probe EW parameters and New Physics!



- observe a pronounced sensitivity to the Weinberg angle, especially low and high x , even at $\mathcal{L} = 100\text{fb}^{-1}$

- this corresponds closely to the kinematics at which EIC is likely to measure A^{PV} — relatively large Q^2 and in the x range $0.2 \lesssim x \lesssim 0.5$

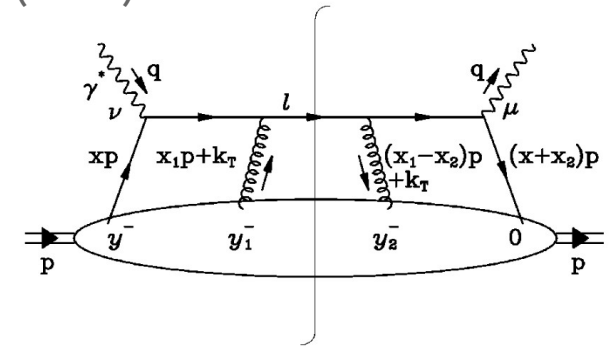
interactions with multiple partons at EIC: nuclear case

- consider jet production in electron-nucleus vs. electron-nucleon DIS

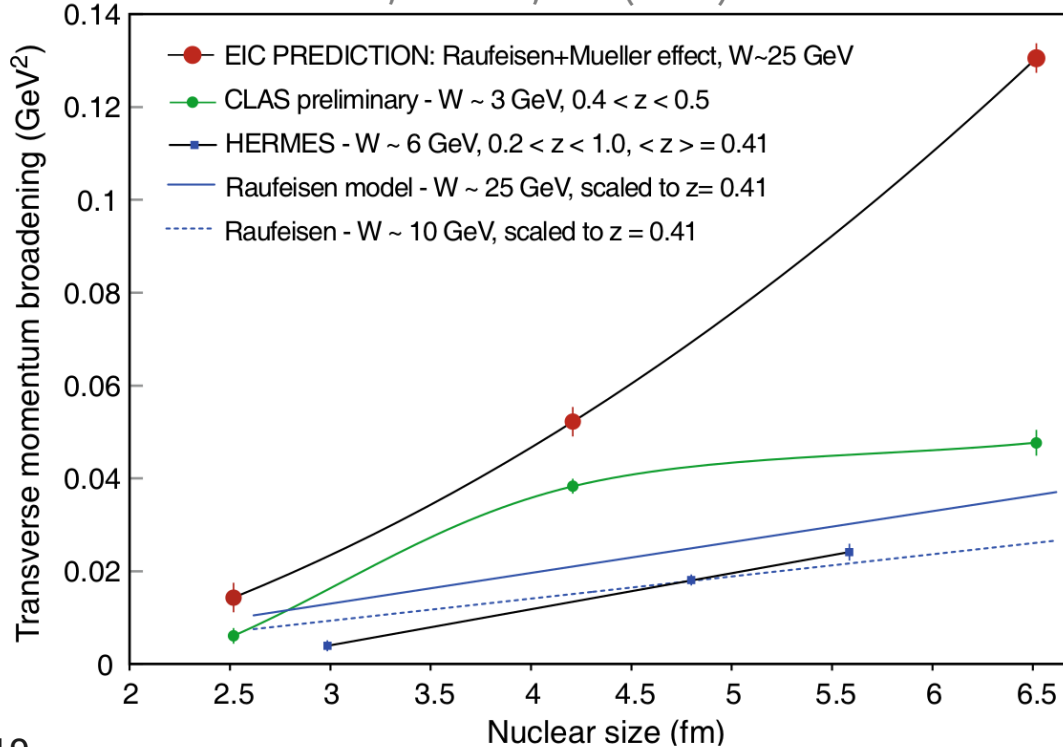
X. Guo, PRD58, 114033 (1998).

$$\Delta \langle p_T^2 \rangle \equiv \langle p_T^2 \rangle_{eA} - \langle p_T^2 \rangle_{ep}$$

$$\langle p_T^2 \rangle = \int dp_T^2 p_T^2 \frac{d\sigma}{dx_B dQ^2 dp_T^2} / \frac{d\sigma}{dx_B dQ^2}$$



Accardi et al., EPJA52, 268 (2016).



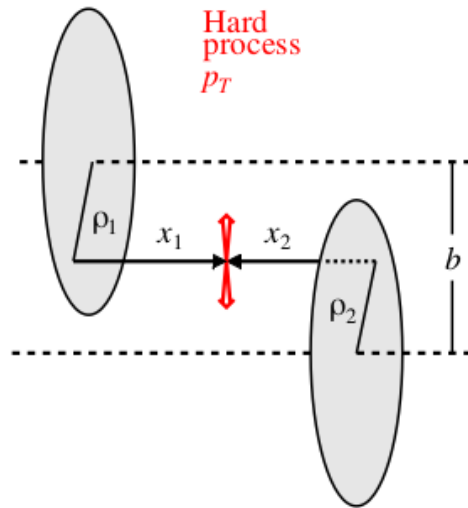
- multi-parton interactions in nuclear scattering:

→ multiple scatterings of produced quark with nuclear medium

→ qualitatively different dependence on nuclear size predicted at EIC energies

→ more phase space for radiation, larger $\Delta \langle p_T^2 \rangle$

Transverse geometry in pp: Hard processes

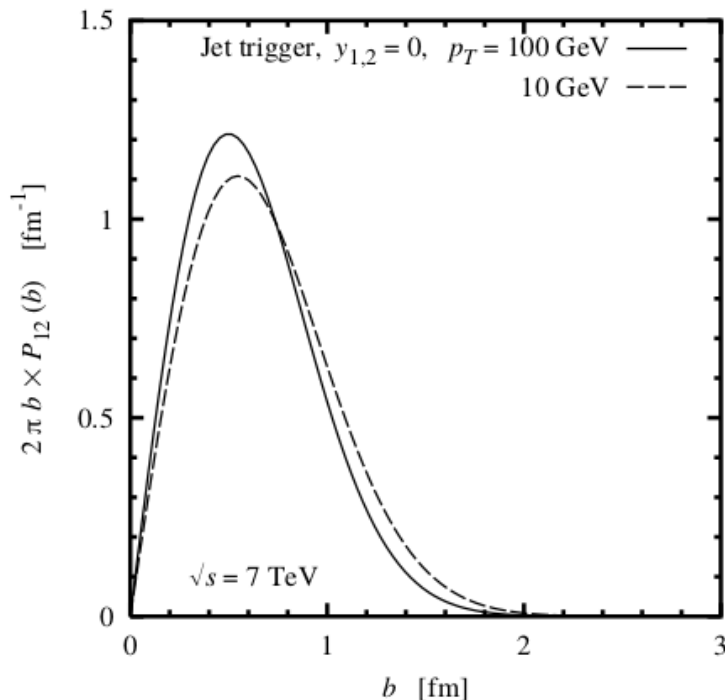


- Hard process from parton-parton collision
Local in transverse space $p_T^2 \gg (\text{transv. size})^{-2}$
- Cross section as function of pp impact par

$$\sigma_{12}(b) = \int d^2\rho_1 d^2\rho_2 \delta(\mathbf{b} - \boldsymbol{\rho}_1 + \boldsymbol{\rho}_2) \times G(x_1, \rho_1) G(x_2, \rho_2) \sigma_{\text{parton}}$$

Thanks to **Christian Weiss!**

→ **precise GPDs furnished by EIC will be crucial!**



Calculable from known transverse distributions
Integral $\int d^2b$ reproduces inclusive formula

Normalized distribn $P_{12}(b) = \sigma_{12}(b) / [\int \sigma_{12}]$

- New information available

Model spectator interactions depending on b
Underlying event

Predict probability of multiple hard processes
Dynamical correlations? FSW04

Diffraction: Gap survival probability
Determined largely by transverse geometry FHSW 07

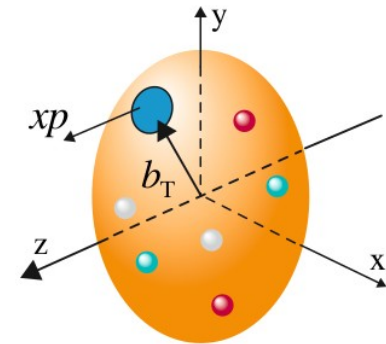
conclusions...

...and the future.

- the commissioning and operation of an EIC is now the priority of the US nuclear and hadronic physics communities

→ the dedicated aim of this effort will be the resolution of long-standing issues in QCD, and the precise determination of the nucleon's multi-dimensional structure

→ the impact of this work will **NOT** be relegated purely to hadronic/nuclear physics!



rather, the expected impact upon high energy physics is substantial

→ controlling SM backgrounds; BSM searches; CGC; **MPIs**; ...

- exploring the physics implications of EIC (including in HEP) requires a **community effort**, esp. to optimize the output of the eventual program

... many opportunities to get involved.



WE WANT YOU!

—— supplementary material ——

the goal is to quantify the strength of the constraints placed on a particular set of PDFs by both individual and aggregated measurements *without direct fitting*

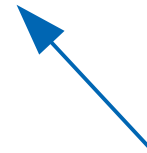
- for single-particle hadroproduction of gauge bosons at, e.g., LHC, factorization gives

$$\sigma(AB \rightarrow W/Z+X) = \sum_n \alpha_s^n(\mu_R^2) \sum_{a,b} \int dx_a dx_b$$

$$\times f_{a/A}(x_a, \mu^2) \hat{\sigma}_{ab \rightarrow W/Z+X}^{(n)}(\hat{s}, \mu^2, \mu_R^2) f_{b/B}(x_b, \mu^2)$$



PDFs determined by fits to data; e.g., "CT14H2"



pQCD matrix elements – specified by theoretical formalism in a given fit

- idea*: study the statistical correlation between PDFs and the quality of the fit at a measured data point(s); fit quality encoded in a (Theory) – (shifted Data) *residual*:

$$r_i(\vec{a}) = \frac{1}{s_i} (T_i(\vec{a}) - D_{i,sh}(\vec{a}))$$

s_i : uncorrelated uncert.

\vec{a} : PDF parameters

a brief statistical aside, i

- the CTEQ-TEA global analysis relies on the Hessian formalism for its error treatment

$$\chi_E^2(\vec{a}) = \sum_{i=1}^{N_{pt}} r_i^2(\vec{a}) + \sum_{\alpha=1}^{N_\lambda} \bar{\lambda}_\alpha^2(\vec{a})$$

← nuisance parameters to handle correlated errors

$$r_i(\vec{a}) = \frac{1}{s_i} (T_i(\vec{a}) - D_{i,sh}(\vec{a}))$$

these result in systematic shifts to data central values:

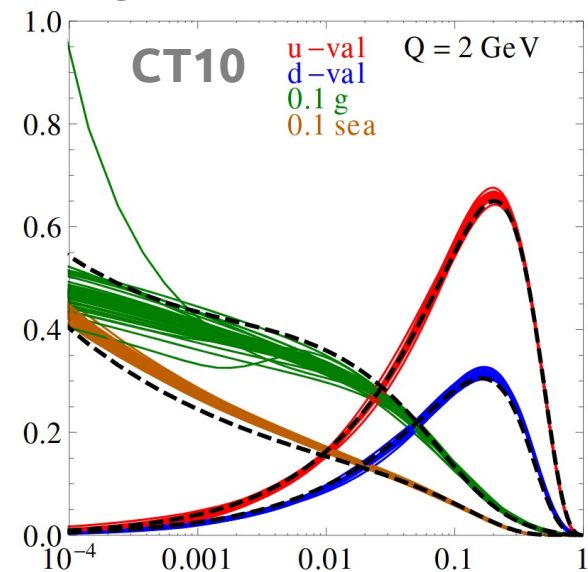
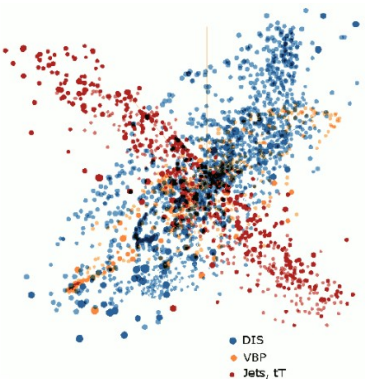
$$D_i \rightarrow D_{i,sh}(\vec{a}) = D_i - \sum_{\alpha=1}^{N_\lambda} \beta_{i\alpha} \bar{\lambda}_\alpha(\vec{a})$$

- a 56-dimensional parametric basis \vec{a} is obtained by diagonalizing the Hessian matrix H determined from χ^2 (following a 28-parameter fit)

use this basis to compute 56-component "normalized" residuals:

$$\delta_{i,l}^\pm \equiv (r_i(\vec{a}_l^\pm) - r_i(\vec{a}_0)) / \langle r_0 \rangle_E$$

where $\langle r_0 \rangle_E \equiv \sqrt{\frac{1}{N_{pt}} \sum_{i=1}^{N_{pt}} r_i^2(\vec{a}_0)}$

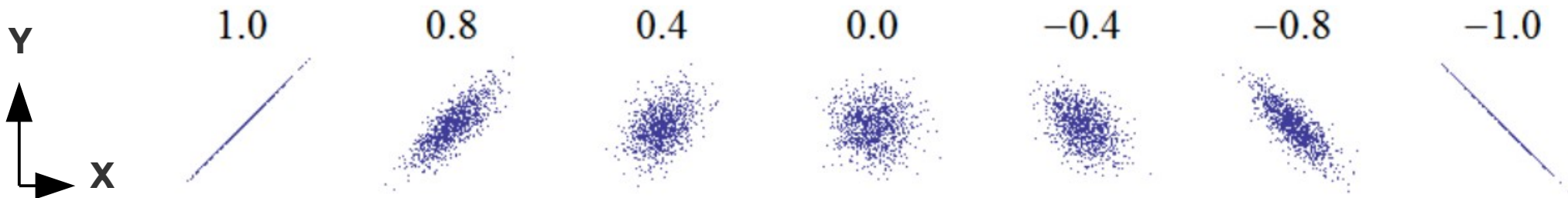


a brief statistical aside, ii

- ... but how does the behavior of these residuals relate to the fitted PDFs and their uncertainties?

for example, how does the PDF uncertainty (at specific x, μ) correlate with the residual associated with a theoretical prediction at the same x, μ ?

examine the Pearson correlation over the 56-member PDF error set between a PDF of given flavor and the residual



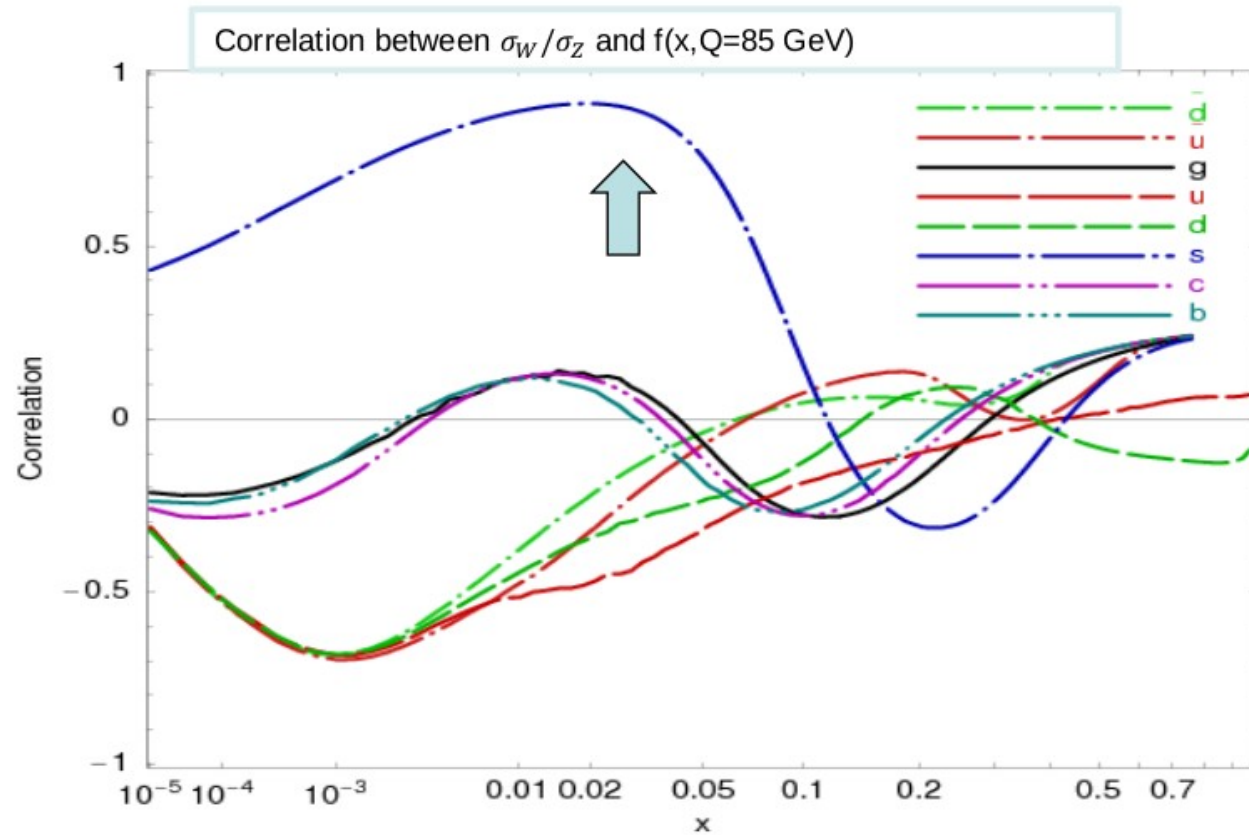
[X,Y] are exactly (anti-)correlated at the far (right) left above.

- we may then evaluate correlations between arbitrary PDF-derived quantities over the ensemble of error sets ([X,Y] may be PDFs, cross sections, residuals,...):

$$\text{Corr}[X, Y] = \frac{1}{4\Delta X \Delta Y} \sum_{j=1}^N (X_j^+ - X_j^-)(Y_j^+ - Y_j^-) \quad \Delta X = \frac{1}{2} \sqrt{\sum_{j=1}^N (X_j^+ - X_j^-)^2}$$

...we may turn to the Pearson correlations between PDFs and δ_i , but we first note

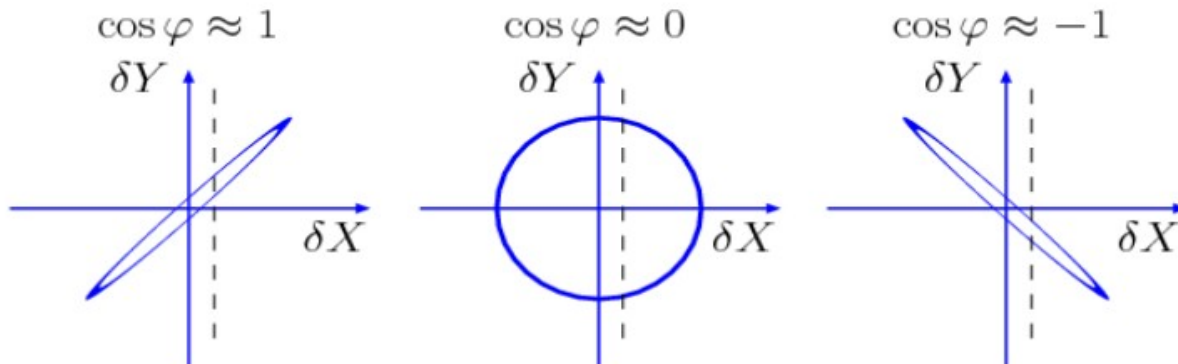
Correlations carry useful, but limited information



CTEQ6.6 [arXiv:0802.0007]:

$\cos \varphi > 0.7$ shows that the ratio σ_W/σ_Z at the LHC must be sensitive to the strange PDF $s(x, Q)$

$\cos \varphi \approx \pm 1$ suggests that a measurement of X **may** impose tight constraints on Y



But, $\text{Corr}[X, Y]$ between **theory** cross sections X and Y does not tell us about **experimental** uncertainties

Correlation C_f and sensitivity S_f

The relation of data point i on the PDF dependence of f can be estimated by:

- $C_f \equiv \text{Corr}[\rho_i(\vec{a}), f(\vec{a})] = \cos\varphi$

$\vec{\rho}_i \equiv \vec{\nabla}r_i / \langle r_0 \rangle_E$ -- gradient of r_i normalized to the r.m.s. average residual in expt E;

$$(\vec{\nabla}r_i)_k = (r_i(\vec{a}_k^+) - r_i(\vec{a}_k^-)) / 2$$

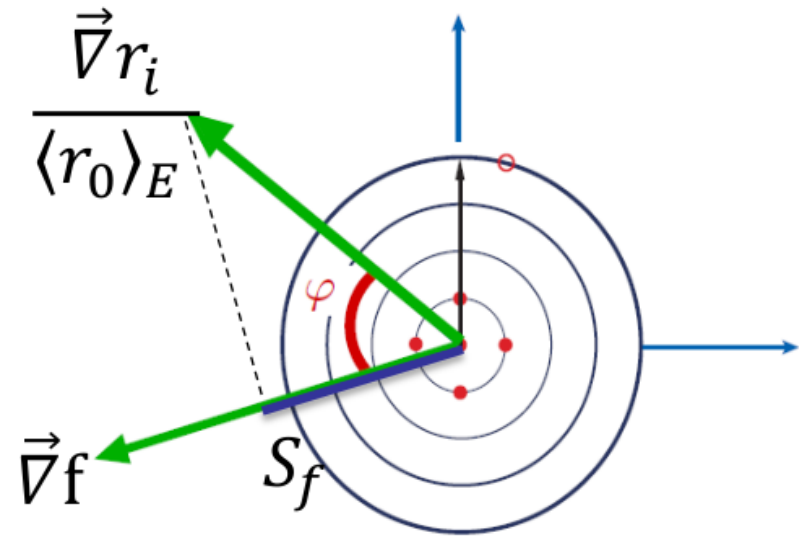
$$\text{Corr}[X, Y] = \frac{1}{4\Delta X \Delta Y} \sum_{j=1}^N (X_j^+ - X_j^-)(Y_j^+ - Y_j^-)$$

C_f is **independent** of the experimental and PDF uncertainties. In the figures, take $|C_f| \gtrsim 0.7$ to indicate a large correlation.

- $S_f \equiv |\vec{\rho}_i| \cos\varphi = C_f \frac{\Delta r_i}{\langle r_0 \rangle_E}$ -- projection of $\vec{\rho}_i(\vec{a})$ on $\vec{\nabla}f$

S_f is proportional to $\cos\varphi$ and the ratio of the PDF uncertainty to the experimental uncertainty. We can sum $|S_f|$.

In the figures, take $|S_f| > 0.25$ to be significant.



2nd aside: kinematical matchings

- residual-PDF correlations and sensitivities are evaluated at parton-level kinematics determined according to leading-order matchings with physical scales in measurements

deeply-inelastic scattering:

$$\mu_i \approx Q|_i, \quad x_i \approx x_B|_i$$

x_i : parton mom. fraction

μ_i : factorization scale

hadron-hadron collisions:

$AB \rightarrow CX$

$$\mu_i \approx Q|_i, \quad x_i^\pm \approx \frac{Q}{\sqrt{s}} \exp(\pm y_C)|_i$$

single-inclusive jet production:

$$Q = 2p_{Tj}, \quad y_C = y_j$$

$t\bar{t}$ pair production:

$$Q = m_{t\bar{t}}, \quad y_C = y_{t\bar{t}}$$

etc...

$d\sigma/dp_T^Z$ measurements:

$$Q = \sqrt{(p_T^Z)^2 + (M_Z)^2}, \quad y_C = y_Z$$

Sensitivity ranking tables

... to assess the impact of separate experiments

No.	Expt.	N_{pt}	Rankings, CT14 HERA2 NNLO PDFs												
			$\sum_f S_f^E $	$\langle \sum_f S_f^E \rangle$	$ S_{\bar{d}}^E $	$\langle S_{\bar{d}}^E \rangle$	$ S_{\bar{u}}^E $	$\langle S_{\bar{u}}^E \rangle$	$ S_g^E $	$\langle S_g^E \rangle$	$ S_u^E $	$\langle S_u^E \rangle$	$ S_d^E $	$\langle S_d^E \rangle$	$ S_s^E $
1	HERAI+II'15	1120.	620.	0.0922	B		A	3	A	3	A	3	B		C
2	CCFR-F3'97	86	218.	0.423	C	1	C	1		3	B	1	C	2	
3	BCDMSp'89	337	184.	0.0908					C		B	3	C		
4	NMCrat'97	123	169.	0.229	C	2					C	2	B	2	
5	BCDMSd'90	250	141.	0.0939	C				C	3	C	3	C	3	
6	CDHSW-F3'91	96	115.	0.199	C	2	C	2		3	C	2	C	3	
7	E605'91	119	113.	0.158	C	2	C	2				3			
8	E866pp'03	184	103.	0.0935		3	C	3			C	3			
9	CCFR-F2'01	69	89.1	0.215		3		3	C	2		3		2	3
10	CMS8jets'17	185	87.6	0.0789					C	3					
11	CDHSW-F2'91	85	82.4	0.162		3		3		3		3	C	3	
12	CMS7jets'13	133	63.8	0.0799					C	3					
13	NuTeV-nu'06	38	58.9	0.259		3		3				3		3	C 1
14	CMS7jets'14	158	57.5	0.0606					C	3					
15	CCFR SI nub'01	38	49.4	0.217		3		3				3		3	C 1
16	ATLAS7jets'15	140	48.2	0.0574						3					
17	CCFR SI nu'01	40	48.	0.2		3		3				3		3	C 1

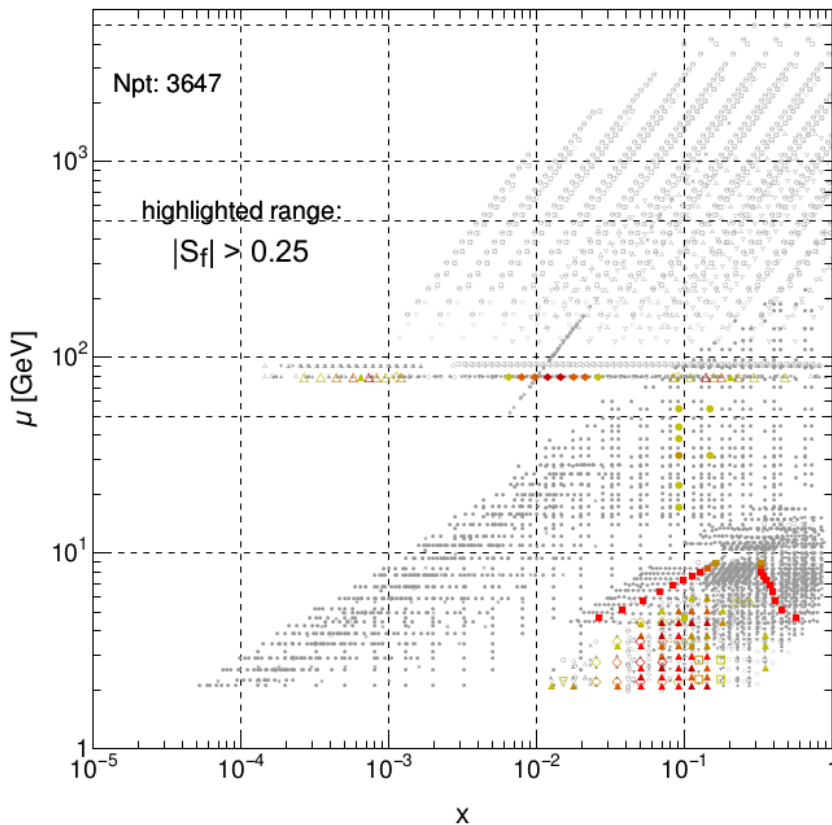
Experiments are listed in the descending order of the summed sensitivities to $\bar{d}, \bar{u}, g, u, d, s$

For each flavor, A and 1 indicate the strongest total sensitivity and strongest sensitivity per point

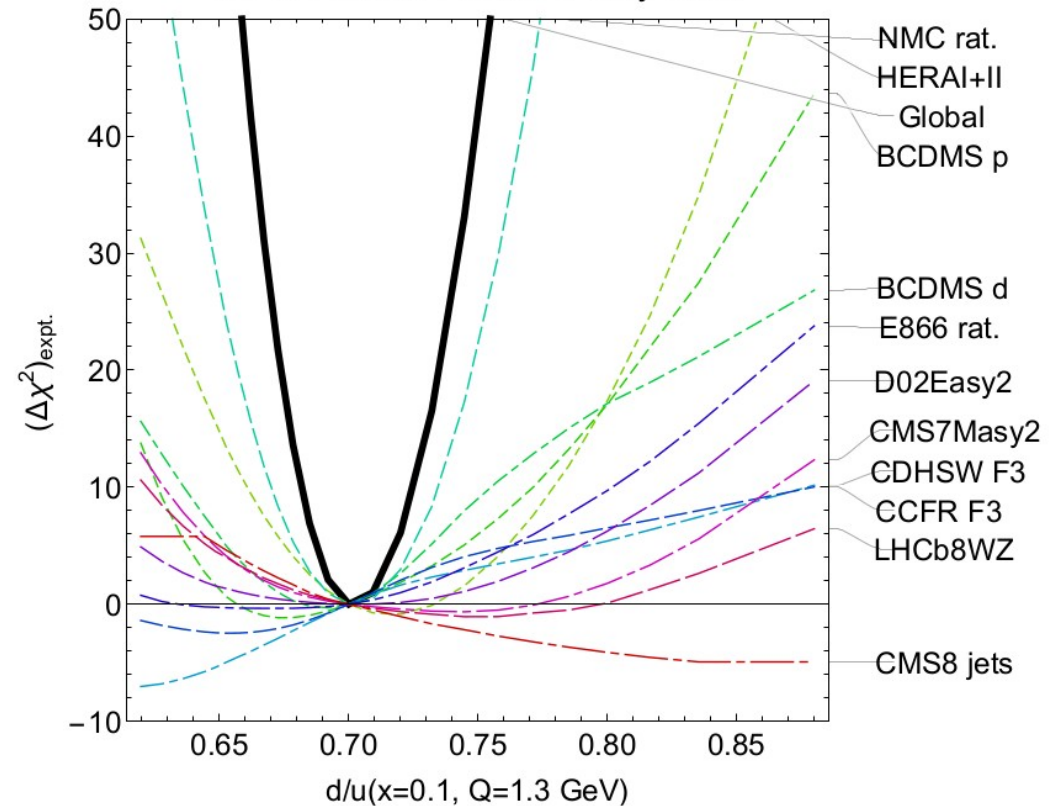
C and 3 indicate marginal sensitivities; low sensitivities are not shown

PDFSense predictions can be validated against actual fits

$|S_f|$ for $d/u(0.1,1.3)$, CT18pre NNLO



CT18 NNLO, + 0.5% theory error



- PDFSense successfully predicts the highest impact data sets *before* fitting, as shown in this illustration for the large x PDF ratio d/u
- Lagrange Multiplier scans provide an independent test of which datasets most drive the global fit in connection with specific PDFs

HERA and fixed-target (BCDMS, NMC) data are dominant!